Backbending phenomena in ^{132,134,136}Ce with a pair-truncated shell model

T. Takahashi[1],* N. Yoshinaga[1],† and K. Higashiyama[1,2]‡
[1]*Department of Physics, Saitama University, Saitama City 338-8570, Japan*
[2]*Department of Physics, University of Tokyo, Hongo, Tokyo 113-0033, Japan*
(Dated: January 3, 2007)

The backbending phenomena observed in Ce isotopes, ^{132,134,136}Ce are investigated in terms of a pair-truncated shell model, a fully microscopic theory which conserves the nucleon number and the total spin. The model reproduces quite well the backbending phenomena, where the experimental bending point of ^{132}Ce is spin 12 and those of ^{134}Ce and ^{136}Ce are spin 10. In addition to high spin states, the theory provides a successful description of energy levels for low-lying collective states as well as those electromagnetic properties, such as $B(E2)$ branching ratios and g factors.

PACS numbers: 21.10.Re, 21.60.Cs, 21.60.Ev, 27.60.+j

I. INTRODUCTION

Many of the nuclei around mass $A = 130$ have an irregular yrast sequence in high-spin states, i.e., the backbending phenomenon. Its basic mechanism is understood as a band crossing between the ground-state band and the s band originating from the alignment of two neutrons in $0h_{11/2}$ orbitals. As a result, sudden decrease of level spacing and $B(E2)$ values around the 10^+_1 states is observed [1–8]. The nuclei in this mass region show another interesting characteristic feature known as the γ instability or weak triaxiality, which becomes manifest in the energy staggering of even-odd spin states in quasi-γ bands and in some forbidden transition rates between yrast and quasi-γ bands.

During the past 20 years, many theoretical studies in the mass $A \sim 130$ region were carried out in terms of various models. A widely used theory for describing even-even nuclei is the interacting boson model (IBM) [9–21]. The low-lying collective states were extensively studied, and the complicated level schemes and electromagnetic properties were well approximated in terms of the O(6) dynamical symmetry of the IBM Hamiltonian. A recent phenomenological study [21], however, indicated that the nuclei around this region might have an intermediate structure between the U(5) and SU(3) limits. Whether the $A \sim 130$ nuclei are described by the O(6) limit or by the U(5)-SU(3) limits remains an open question. A similar study was made using the fermion dynamical symmetry model [22–24], where the even-even nuclear states were constructed by angular momenta zero (S) and two (D) collective pairs. This approach also reproduced some properties of the low-lying states. However, the model has deficiencies that structure of pairs is fixed irrespective of dynamics, and that the contribution of single-particle energies is a constant.

There exist other theoretical investigations, such as the SD version of the pair-truncated shell model (PTSM) [25–30] and the nucleon-pair shell model (NPSM) [31]. In Refs. [32–34], the NPSM was applied to even-even nuclei around $A \sim 130$, and the result gives a good agreement to the experimental energy levels and electromagnetic properties. Recently, systematic studies have been carried out for the $A \sim 130$ nuclei in the context of the PTSM [30]. In this study, the effective interaction consists of single particle energies, and the monopole and quadrupole pairing plus quadrupole-quadrupole (P+QQ) interactions, whose strengths are assumed to be smoothly changed as functions of the number of valence neutrons and/or protons. Spectra of both yrast and quasi-γ bands for even-even Xe, Ba, Ce and Nd isotopes were reproduced very well, along with intraband and interband $B(E2)$ values. The same set of interactions was simply applied to odd-mass nuclei, and an excellent agreement with experiment for both energy spectra and magnetic moments was given.

The most approaches for analyzing the backbending phenomena in well-deformed rare-earth nuclei are based on mean field frameworks. Various Hartree-Fock-Bogoliubov (HFB) calculations using the P+QQ interactions described the backbending phenomena successfully [35–38]. On the other hand, in the $A \sim 130$ region there was no study in terms of the mean field theories, since these approaches cannot adequately describe the transitional nuclei. Thus, very few theoretical approaches were made for the $A \sim 130$ nuclei. For example, a full-fledged shell model calculation for Xe isotopes, $^{130-136}$Xe was carried out under the assumption of $N = Z = 64$ subshell closure [39]. This was a first attempt to describe both low-lying collective states and backbending phenomena at high spin on the same footing using a shell model. Quantum-number-projected generator coordinate method calculations for ^{130,132}Xe were also carried out under the same circumstance as the shell model calculation [40]. The result shows that the γ degree of freedom plays an important role in describing these nuclei, especially for the quasi-γ bands.

The sd-IBM which has only s and d bosons as ingredients, cannot describe the backbending phenomena, since they have no room to take the spin-aligned two-

*Electronic address: takahasi@phy.saitama-u.ac.jp
†Electronic address: yoshinaga@phy.saitama-u.ac.jp
‡Electronic address: higashi@nt.phys.s.u-tokyo.ac.jp

quasiparticle configurations into account. A few studies were made using an extended IBM, where one of the IBM bosons is replaced by a pair of nucleons at high spin [41–44]. For the same reason, the SD version of the PTSM is inadequate for a description of high spin states. Thus, the SD+H version of the PTSM was proposed to describe both low-lying collective states and backbending phenomena at high spin on the same footing [45], where the SD pair truncation scheme is extended to include the H-pair, which is made of two $0h_{11/2}$ nucleons. The model was applied to ^{132}Ba, and the results were in excellent agreement with experiment. Recently the PTSM has been extended for an application to odd-odd nuclei. The model has denied the notion of chiral bands appearing in low-lying states and revealed that the yrast and yrare bands are not chiral partners [46].

The isotopic chain of Ce isotopes with $N \leq 82$ is of great interest in nuclear structure physics because of the following reasons. Both low-lying collective states and backbending phenomena were studied experimentally in an extensive way. The backbending occurs at spin 10 in ^{134,136}Ce, and at spin 12 in ^{132}Ce. Furthermore, the magnetic rotation bands are observed in ^{134,136}Ce [7, 47, 48], and the superdeformed bands, in ^{132}Ce [49, 50]. A lot of theoretical investigations were also carried out on these isotopes. There were some studies on the low-lying states for Ce isotopes in terms of the IBM [11, 12], the NPSM within the SD subspace [33] and the SD version of the PTSM [30], as mentioned above. For a description of the backbending phenomena, the extended IBM calculation was also made [42]. The superdeformed bands of ^{132}Ce were studied by use of the cranked HFB model [36], and energy levels and electromagnetic properties were well investigated.

In this paper, we use the SD+H version of the PTSM to calculate the energy spectra for ^{132,134,136}Ce using the P+QQ interaction as an effective interaction. The $E2$ transition rates are calculated to give the results which are almost identical to the O(6) limit of the IBM and g factors are also calculated and predicted. The paper is organized as follows. In Sec. II, the framework of the PTSM and its model space are described. In Sec. III, the PTSM calculations are carried out for ^{132,134,136}Ce. The results are summarized in Sec. IV.

II. THEORETICAL FRAMEWORK

The nuclear shell model remains one of the most fundamental approaches for a microscopic description of nuclear structure. It has been very successful to understand the structure of light nuclei. On the other hand, the model cannot be immediately applied to medium and heavy nuclei except a few nuclei lying near a shell closure. The main difficulty is the uncontrollable problem of dimension explosion. In order to avoid this problem, we must accept some kind of truncation schemes. In the SD version of the PTSM, the shell model basis is restricted to the SD subspace with S and D being collective pairs. The S and D pair creation operators are defined as

$$S^\dagger = \sum_j \alpha_j A_0^{\dagger(0)}(jj), \tag{1}$$

$$D_M^\dagger = \sum_{j_1 j_2} \beta_{j_1 j_2} A_M^{\dagger(2)}(j_1 j_2), \tag{2}$$

where the structure coefficients α and β are obtained by means of the variational procedure in the present approach. The creation operator of a pair of nucleons in orbitals j_1 and j_2 with total angular momentum J, and its projection M is given by

$$A_M^{\dagger(J)}(j_1 j_2) = [c_{j_1}^\dagger c_{j_2}^\dagger]_M^{(J)}, \tag{3}$$

where $c_j^\dagger$ represents either a neutron-hole creation operator or a proton-particle creation operator in an orbital j. The collective states of even-even nuclei are created by applying the S and D pair-creation operators to the closed-shell core $|-\rangle$:

$$|\Phi(I\eta)\rangle = (S^\dagger)^{n_s}(D^\dagger)^{n_d}\,|-\rangle\,, \tag{4}$$

where I is a total spin of the nuclear state, and η, an additional quantum number required to uniquely specify the state. Here, the necessary angular momentum coupling is exactly carried out, but abbreviated for notational simplicity. The number of valence nucleon pairs, $n_s + n_d$, is fixed constant for a specific nucleus, representing half the number of valence nucleons. The validity of the SD subspace approximation has been thoroughly investigated in Refs. [25–30].

As studied in the previous experimental studies [1, 2], the yrast bands of several $A \sim 130$ nuclei show an anomalous behavior of level spacing at high spins, which arise due to the band crossing between the ground-state band and the aligned neutron $(0h_{11/2})^2$ band, s band. For the description of them, we need to extend the SD version of the PTSM so as to accommodate the low-lying states and the backbending phenomena, simultaneously. In the SD+H version of the PTSM, a pair of nucleons in the $0h_{11/2}$ orbital is introduced in addition to the ordinary S and D pairs. This model is regarded as an improvement of the extended IBM by replacing all the core bosons with explicit fermionic pairs.

The H-pair creation operator is defined as

$$H_M^\dagger = [c_{11/2}^\dagger\, c_{11/2}^\dagger]_M^{(10)}, \tag{5}$$

where two nucleons in $0h_{11/2}$ orbitals can even couple to angular momenta other than spin J=10, but the J=10 pair is assumed to be most important. In contrast to the S and D pairs, the H pair is non-collective, since it has a unique structure consisting of $0h_{11/2}$ orbitals. Then, the SD+H pair state is written by

$$|\Phi(I\eta)\rangle = (S^\dagger)^{n_s}(D^\dagger)^{n_d}(H^\dagger)^{n_h}\,|-\rangle\,, \tag{6}$$

where I and η denote the same as before, and $2(n_s+n_d+n_h)$ gives the number of valence nucleons. Here angular momentum coupling is exactly carried out, but it is abbreviated to denote as before. In the present calculation, the number of the H pairs is limited to one (i.e., $n_h = 1$) for each kind of nucleon space. This state contributes to describing nuclear states of even-even nuclei, in addition to the states given by Eq. (4). Through Schmidt ortho-normalization procedure, states of Eqs. (4) and (6) are ortho-normalized to each other in neutron or proton space with a total spin I.

In this present study, we employ the P+QQ interaction as an effective interaction, which is frequently used for medium and heavy nuclei. The effective shell model Hamiltonian is written as

$$H = H_\nu + H_\pi + H_{\nu\pi}, \tag{7}$$

where H_ν, H_π and $H_{\nu\pi}$ represent the neutron interaction, the proton interaction and the neutron-proton interaction, respectively. The interaction among like nucleons H_τ ($\tau = \nu$ or π) consists of spherical single-particle energies, the monopole-pairing (MP) interaction, the quadrupole-pairing (QP) interaction, and the quadrupole-quadrupole (QQ) interaction:

$$\begin{aligned} H_\tau &= \sum_{jm} \epsilon_{j\tau} c^\dagger_{jm\tau} c_{jm\tau} - G_{0\tau} P^{\dagger(0)}_\tau P^{(0)}_\tau \\ &\quad -G_{2\tau} P^{\dagger(2)}_\tau \cdot \tilde{P}^{(2)}_\tau - \kappa_\tau : Q_\tau \cdot Q_\tau :, \end{aligned} \tag{8}$$

where :: denotes normal ordering. Here the monopole-pairing operator $P^{\dagger(0)}_\tau$, the quadrupole-pairing operators $P^{\dagger(2)}_{M\tau}, \tilde{P}^{\dagger(2)}_{M\tau}$ and the quadrupole operator $Q_{M\tau}$ are defined as

$$P^{\dagger(0)}_\tau = \sum_j \frac{\sqrt{2j+1}}{2} A^{\dagger(0)}_{0\tau}(jj), \tag{9}$$

$$P^{\dagger(2)}_{M\tau} = \sum_{j_1 j_2} Q_{j_1 j_2} A^{\dagger(2)}_{M\tau}(j_1 j_2), \tag{10}$$

$$\tilde{P}^{(2)}_{M\tau} = (-)^M P^{(2)}_{-M\tau}, \tag{11}$$

$$Q_{M\tau} = \sum_{j_1 j_2} Q_{j_1 j_2} \left[c^\dagger_{j_1\tau} \tilde{c}_{j_2\tau} \right]^{(2)}_M, \tag{12}$$

$$(\tilde{c}_{jm\tau} = (-1)^{j-m} c_{j-m\tau}),$$

$$Q_{j_1 j_2} = -\frac{\langle j_1 \| r^2 Y^{(2)} \| j_2 \rangle}{\sqrt{5}}, \tag{13}$$

where $A^{\dagger(J)}_{M\tau}(j_1 j_2)$ stands for the creation operator of a pair of nucleons defined in Eq. (3). We assume that the interaction between neutrons and protons $H_{\nu\pi}$ is just given by the QQ interaction,

$$H_{\nu\pi} = -\kappa_{\nu\pi} Q_\nu \cdot Q_\pi, \tag{14}$$

where the neutron quadrupole operator Q_ν is written in terms of neutron-hole operators. As for the single-particle basis states, the harmonic oscillator basis states with the oscillator parameter $b = \sqrt{\hbar/M\omega}$ are employed.

TABLE I: Adopted single-particle energies for neutron holes and proton particles, which are extracted from experiment [51–53] (in MeV).

j	$2s_{1/2}$	$0h_{11/2}$	$1d_{3/2}$	$1d_{5/2}$	$0g_{7/2}$
ε_ν	0.332	0.242	0.000	1.655	2.434
ε_π	2.990	2.793	2.708	0.962	0.000

TABLE II: Adopted strengths of the MP interactions (in MeV), QP and QQ interactions (both in MeV/b^4) for ^{132,134,136}Ce.

Nucleus	$G_{0\nu}$	$G_{2\nu}$	κ_ν	$G_{0\pi}$	$G_{2\pi}$	κ_π	$\kappa_{\nu\pi}$
^{132}Ce	0.150	0.048	0.110	0.110	0.030	0.035	−0.110
^{134}Ce	0.150	0.044	0.110	0.115	0.025	0.035	−0.110
^{136}Ce	0.150	0.040	0.110	0.120	0.020	0.035	−0.110

III. NUMERICAL RESULTS

The Ce isotopes of mass $A \sim 130$ region have 8 valence protons outside the closed shell $Z = 50$ and several neutron holes with respect to the closed shell $N = 82$. Since the valence neutron holes and proton particles occupy the $0g_{7/2}$, $1d_{5/2}$, $1d_{3/2}$, $0h_{11/2}$, and $2s_{1/2}$ orbitals, we take the full $50 \sim 82$ configuration spaces for both neutrons and protons. The adopted single-particle energies are listed in Table I, which are extracted from experimental excitation energies in Refs. [51–53]. In this study valence neutrons are treated as holes and valence protons, as particles.

The adopted strengths of the MP, QP and QQ interactions are shown in Table II. These interaction strengths are adjusted so as to reproduce the experimental excitation energies of the 2^+_1, 4^+_1, 6^+_1, 8^+_1, 10^+_1 and 12^+_1 states in the yrast band, and the 2^+_2, 3^+_1, 4^+_2 and 5^+_1 states in the quasi-γ band. Here we neglect the levels which are not experimentally confirmed. Furthermore, the force strengths, $G_{0\tau}$, $G_{2\tau}$, κ_τ and $\kappa_{\nu\pi}$, are assumed to have a linear dependence on the number of valence nucleons. Although the force strengths of the neutron MP interaction $G_{0\nu}$ are the same for all the Ce isotopes, those of the proton MP interaction $G_{0\pi}$ and both neutron and proton QP interaction $G_{2\nu}$, $G_{2\pi}$ are changed as functions of the neutron number. This dependence is necessary to obtain a better agreement between the theoretical energy levels and experimental data for Ce isotopes. As discussed later, proton quadrupole excitations play important roles in the low-lying structure of these nuclei. In order to describe complicated level schemes for each nucleus, we need to slightly change the force strengths of the proton MP interaction.

The SD+H version of the PTSM was first applied to ^{132}Ba, where the backbending phenomenon was well reproduced [45]. The MP interactions of the present study are smaller than those used in ^{132}Ba, where (in MeV) $G_{0\nu} = 0.150$, and $G_{0\pi} = 0.170$ were used. As compared

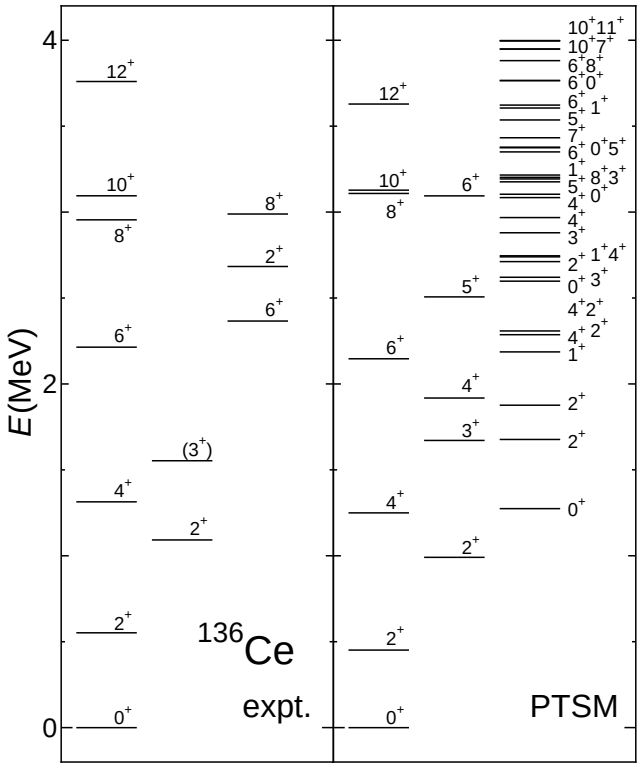

FIG. 1: Comparison of experimental energy spectrum (expt.) with the PTSM results (PTSM) for ^{136}Ce. The experimental data are taken from Ref. [7, 56].

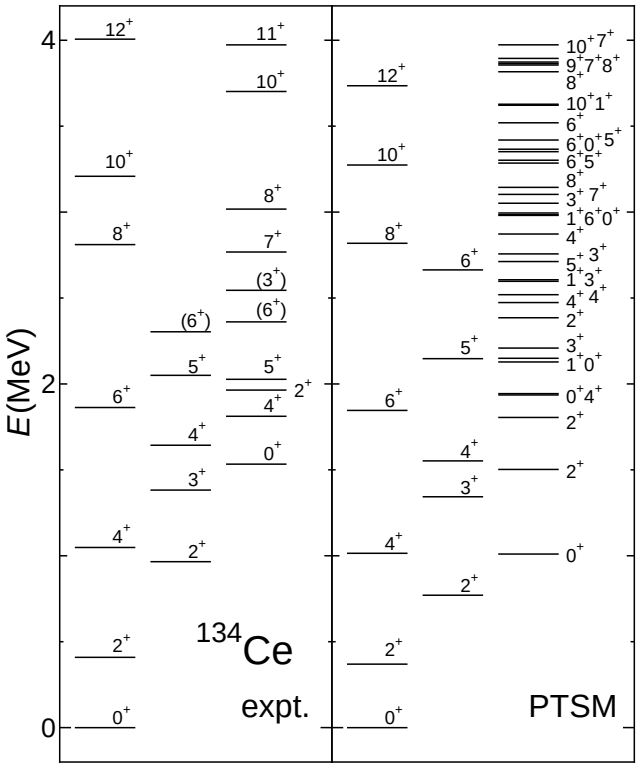

FIG. 2: Comparison of experimental energy spectrum (expt.) with the PTSM results (PTSM) for ^{134}Ce. The experimental data are taken from Ref. [4, 57].

to other previous studies [33, 54], the force strengths of the MP interaction are also smaller. For instance, the NPSM calculation in the SD space [33] uses $G_{0\nu} = 0.180$, and $G_{0\pi} = 0.131$. In Ref. [54], the values $G_{0\nu} = G_{0\pi} = 23/A$ MeV were used for nuclei in the $A \sim 130$ region. If we use such larger strengths of the MP interactions, our theory cannot reproduce both experimental energy spectra and some electromagnetic transition rates, simultaneously.

The energy spectra obtained by the PTSM are shown on the right side in Figs. 1–3. On the left side are experimental levels taken from Refs. [4, 7, 11, 56–59]. For construction of the level scheme of the quasi-γ band, we take the state with spin I, which has the largest $E2$ transition rate to the state with spin $I-2$. In ^{136}Ce, the level spacing between the yrast 8^+ and 10^+ states is very small in experiment (140 keV [7]). Our theoretical energy levels match the irregularity of the experimental data (19.1 keV). Although the theoretical level spacing between the 2_2^+ and 3_1^+ states on the quasi-γ band is a bit larger than experiment, the relative positions of the 2_2^+ and 3_1^+ states to the yrast states are well described. Our theoretical result shows the energy staggering of even-odd spin states on the quasi-γ band, which indicates the γ instability in low-lying states. In ^{134}Ce, the even-spin yrast sequence is well reproduced except for the 12^+ state, which is lower than experiment. The calculated quasi-γ band appears somewhat lower in energy than experiment, but the 5_1^+ and 6_2^+ states are higher in energy. However, our results give a good description of the staggering seen in 2_2^+, 3_1^+, 4_2^+, and 5_1^+ states in the quasi-γ band. In ^{132}Ce, experimental level spacing between the 8_1^+ and 10_1^+ states becomes large. On the contrary the spacing between the 10_1^+ and 12_1^+ states becomes small, which is in contrast with the cases for ^{136}Ce and ^{134}Ce. In spite of the differences in energy levels between ^{132}Ce and the others, our calculation reproduces quite well the behavior of the energy levels for the yrast band. Like ^{134}Ce, the even-odd staggering in the quasi-γ band is well reproduced. The yrast states of Ce isotopes were also studied by the extended IBM [42], and good results were obtained like ours.

The backbending phenomena can be clearly seen in the so-called backbending plot. Experimental γ-ray energies versus spin I are compared with the PTSM results along the yrast sequence in Fig. 4. For ^{132}Ce and ^{136}Ce, the calculated levels agree quite well with experimental ones, especially our calculations successfully reproduce the sudden decrease of level spacing occurring between the 10_1^+ and 12_1^+ states for ^{132}Ce, and between the 8_1^+ and 10_1^+ states for ^{136}Ce. In case of ^{134}Ce, the experimental level spacing between the 8_1^+ and 10_1^+ states is small. On the other hand, our calculation provides the undesired results; the both level spacings between the 8_1^+

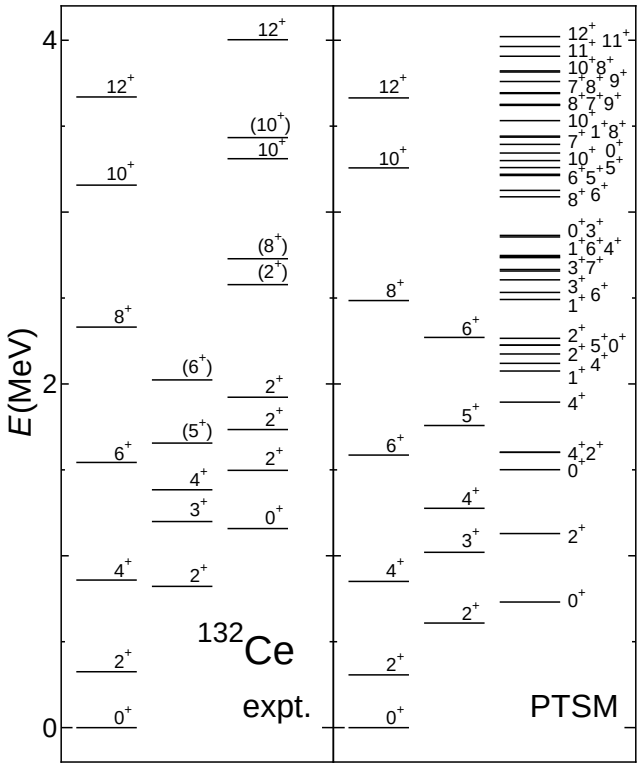

FIG. 3: Comparison of experimental energy spectrum (expt.) with the PTSM results (PTSM) for ^{132}Ce. The experimental data are taken from Ref. [11, 58, 59].

and 10_1^+ states and between the 10_1^+ and 12_1^+ states are small. It is difficult to produce such a rapid change as seen in experiment when changing from ^{136}Ce to ^{132}Ce, since in the present study the strengths of effective interactions are assumed to be linear functions of the valence neutron number.

The $E2$ transition operator is defined as

$$T(E2;\mu) = e_\nu Q_{\nu\mu} + e_\pi Q_{\pi\mu}, \tag{15}$$

where e_τ represents the effective charge of the nucleon, and the operator Q_τ is the quadrupole operator defined in Eq. (12). As for the effective charges, we use e_ν=−1.2 e and e_π=+2.2 e, in accordance with the conventional relation e_ν=$-\delta e$ and e_π=$(1+\delta)e$ [55]. They are fixed so as to reproduce the experimental $B(E2;2_1^+ \to 0_1^+)$ value of ^{134}Ce. Note that the neutron effective charge is chosen to be negative, as valence neutrons are treated as holes. In Fig. 5, calculated $B(E2)$ values in the yrast band are compared with the experimental data. We can reproduce the $B(E2;2_1^+ \to 0_1^+)$ value for ^{136}Ce, and the $B(E2;10_1^+ \to 8_1^+)$ values for ^{132}Ce and ^{134}Ce. However, there are many disagreements between the theoretical $B(E2)$ values and experimental data. In particular, for all Ce isotopes the experimental $B(E2)$ values for $4_1^+ \to 2_1^+$ transition are smaller than those for $2_1^+ \to 0_1^+$ transition, while the opposite behavior is shown in the PTSM result. We suspect that experimental data might be erroneous, because theoretically we believe that it is impossible to produce a smaller value for $B(E2;4_1^+ \to 2_1^+)$ than $B(E2;2_1^+ \to 0_1^+)$ in any existing collective models.

For instance, let us consider the results of the IBM1 which is well known to explain several properties of a wide variety of medium and heavy nuclei. In the model, we have three dynamical symmetry limits, the U(5), the SU(3) and the O(6) limits, which well describe rotational nuclei, vibrational nuclei and γ-soft nuclei, respectively. For each limit, we derive the formulae for the $B(E2;4_1^+ \to 2_1^+)/B(E2;2_1^+ \to 0_1^+)$ ratios [see Ref. [9], Eq. (2.140)]:

$$\frac{B(E2;4_1^+ \to 2_1^+)}{B(E2;2_1^+ \to 0_1^+)} = \begin{cases} 2\dfrac{(N-1)}{N} & \text{[for U(5)]} \\ \dfrac{10}{7}\dfrac{(N-1)(2N+5)}{N(2N+3)} & \text{[for SU(3)]} \\ \dfrac{10}{7}\dfrac{(N-1)(N+5)}{N(N+4)} & \text{[for O(6)]} \end{cases}, \tag{16}$$

where N is half the number of valence nucleons. For larger N, the ratios of 2, 10/7 and 10/7 are obtained for the U(5), the SU(3) and the O(6) limits, respectively. The IBM always predicts that the $B(E2;4_1^+ \to 2_1^+)$ is larger than the $B(E2;2_1^+ \to 0_1^+)$. Thus this anomalous behavior of $B(E2)$ values cannot be explained also by the IBM.

A feature of the backbending is manifested as an appearance of a sudden drop in the experimental $B(E2)$ values, and such a behavior is well simulated by the PTSM. It should be noted that our calculations give rapid drops of the $B(E2)$ values at spin 10 for all nuclei ^{132,134,136}Ce. Although the level spacing between the 8_1^+ and 10_1^+ states is large for ^{132}Ce, the $B(E2)$ value of the $10_1^+ \to 8_1^+$ transition is very small. It indicates that the internal structure drastically changes from the 8_1^+ to the 10_1^+ states. It is inferred that the basic structure is the same for all Ce isotopes although they have backbending occurring at different angular momenta.

In Table III, the relative $B(E2)$ values in low-lying states calculated for ^{132,134,136}Ce are compared with experiment, and also with the O(6) limit of the IBM. For ^{134}Ce and ^{132}Ce, good agreements between theoretical relative $B(E2)$ values and experimental data are achieved. Especially, forbidden $E2$ interband transition rates are well reproduced. Note that no experimental data are available for ^{136}Ce. The PTSM predicts the results very close to the O(6) limit, which is known to describe γ-unstable nuclei.

The magnetic dipole operator is given by

$$\boldsymbol{\mu} \;=\; \mu_N \sum_{\tau=\nu,\pi} [g_{\ell\tau}\boldsymbol{j}_\tau + (g_{s\tau} - g_{\ell\tau})\boldsymbol{s}_\tau], \tag{17}$$

where μ_N $(= e\hbar/2mc)$ is the nuclear magneton, and $g_{\ell\tau}$ $(g_{s\tau})$ is the gyromagnetic ratio for the orbital angular

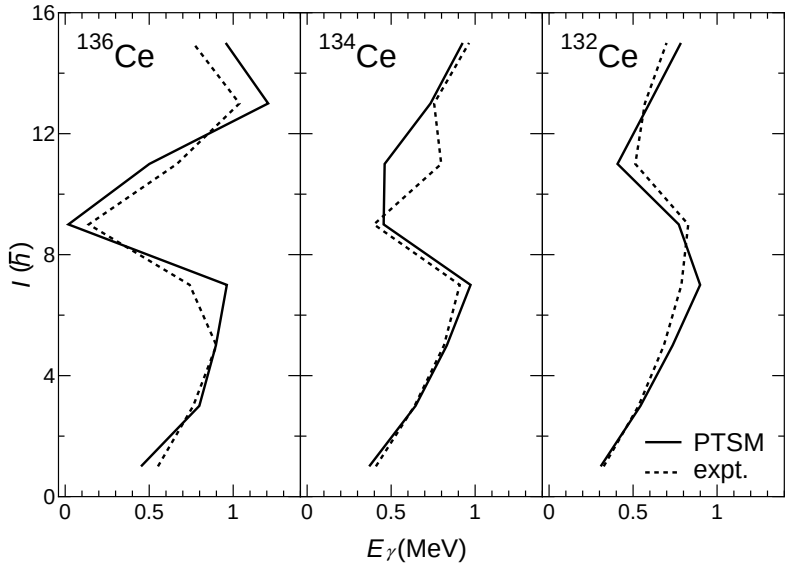

FIG. 4: Comparison of γ-ray energies $E_\gamma[E_\gamma = E(I+1) - E(I-1)]$ versus angular momentum I in experiment (expt.) with the PTSM results (PTSM) for ^{132,134,136}Ce. The experimental data are taken from Refs. [4, 7, 58].

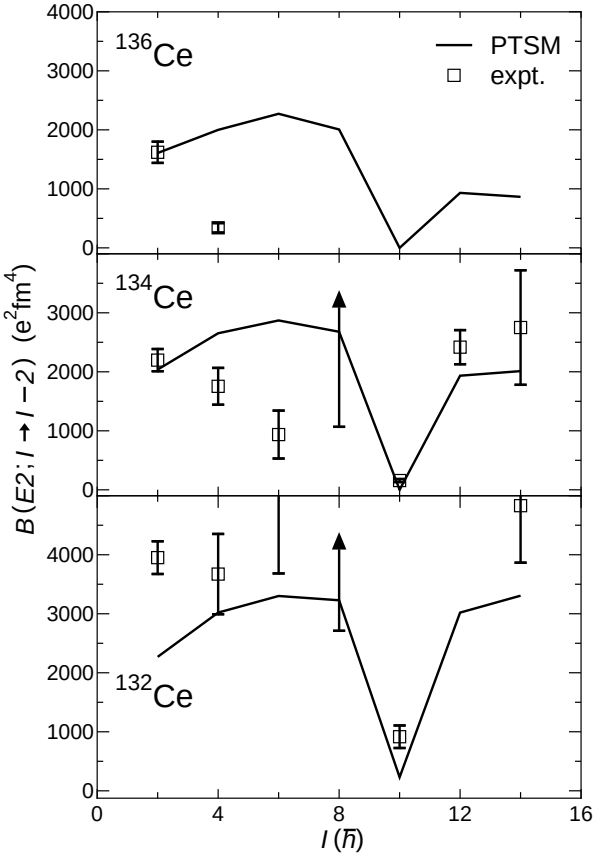

FIG. 5: Comparison of the yrast $B(E2)$ values in the PTSM (PTSM) with the experimental data (expt.) for ^{132,134,136}Ce. The experimental data are taken from Refs. [60–62].

TABLE III: Comparison of calculated relative $B(E2)$ values for ^{132,134,136}Ce, experimental data (expt.), and the prediction of O(6) limit of the IBM. The experimental data are taken from Refs. [11, 57]. No experimental data are available for ^{136}Ce.

	^{132}Ce		^{134}Ce		^{136}Ce	O(6)
$J_i^\pi \to J_f^\pi$	PTSM	expt.	PTSM	expt.	PTSM	
$2_2^+ \to 2_1^+$	100	100	100	100	100	100
$\to 0_1^+$	1.5	6.1	1.1	5.4	3.1	0
$3_1^+ \to 2_2^+$	100	100	100	100	100	100
$\to 4_1^+$	54	29.1(7)	50	25.0	48	40
$\to 2_1^+$	1.4	4.0	0.75	2.2	2.5	0
$4_2^+ \to 2_2^+$	100	100	100	100	100	100
$\to 3_1^+$	6.6		0.039		1.5	0
$\to 4_1^+$	68	59	72	55.0	68	91
$\to 2_1^+$	0.70	0.42	1.5	0.63	5.3	0
$0_2^+ \to 2_2^+$	100	100	100	100	100	100
$\to 2_1^+$	1.7	0.56	2.0	$\leqslant$2.7	4.8	0

momentum (spin). The operators $\boldsymbol{j}_\tau$ and $\boldsymbol{s}_\tau$ stand for the angular momentum and spin operators, respectively. The adopted gyromagnetic ratios for orbital angular momenta are $g_{\ell\nu} = 0.00$, $g_{\ell\pi} = 1.00$, and those for spins are $g_{s\nu} = -2.68$ and $g_{s\pi} = 3.91$, which are free nucleon g factors attenuated by a factor of 0.7. The theoretical results of g factors of the even-spin yrast states are shown in Fig. 6 together with the observed g factors of the 10_1^+ states. For all Ce isotopes, the g-factor along the even-spin yrast line slightly increases as spin I goes up to 8, and drops suddenly at spin 10. The negative values of the g factor reflect the alignment of the $0h_{11/2}$ neutrons. These results are similar to the previous PTSM calculation for ^{132}Ba [45]. With respect to the 10_2^+ states

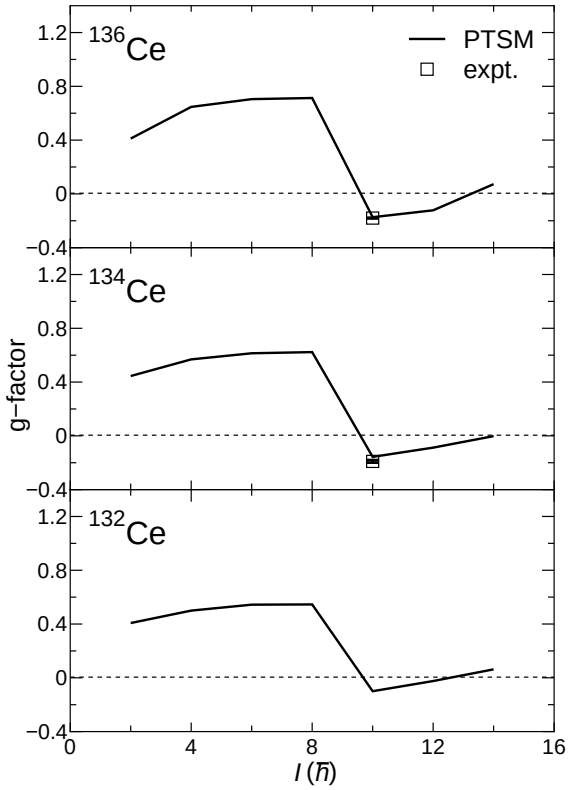

FIG. 6: Comparison of the calculated g factors in the PTSM (PTSM) with the measured values in the yrast states (expt.) for ^{132,134,136}Ce. The experimental data are taken from Refs. [2, 63].

appearing at 3300, 3620, 3950 keV in theory, we obtain the g-factors of +1.23, +1.24 and +1.29 for ^{132}Ce, ^{134}Ce and ^{136}Ce, respectively. The large positive g-factors indicate that the theoretically predicted 10_2^+ states have the alignment of two $0h_{11/2}$ protons.

The internal changes of the structure for Ce isotopes can be seen by inspecting the expectation values of the number of D_τ and H_τ pairs, which are shown as functions of spin I in Fig. 7. For every nucleus, the S and D pairs are dominant in the states up to spin 8, so that the SD truncation scheme works well for the description of low-lying states. Furthermore, since the number of the proton D (D_π) pairs rapidly increases compared to that of the neutron D (D_ν) pairs, the proton quadrupole excitations are responsible for the low-lying states especially for ^{136}Ce. This interpretation is consistent with the previous PTSM calculation for ^{132}Ba [45]. Above spin 10, the sudden increase of the neutron H (H_ν) pair implies that decoupling of two $0h_{11/2}$ neutrons yields the backbending. ¿From the results of the $E2$ transitions, it is found that the internal structure of ^{132}Ce drastically changes when spin increases from 8 to 10. A similar thing is also confirmed in the expectation values of the number of the D and H pairs. This concludes that for ^{132}Ce the internal structure drastically changes from the 8_1^+ to the 10_1^+ states like the other nuclei.

IV. SUMMARY

In this paper the level schemes and electromagnetic properties observed in ^{132,134,136}Ce were investigated in terms of the SD+H version of the pair-truncated shell model (PTSM). In the model, the shell model basis is restricted to the SD+H subspace where the S and D collective pairs and non-collective $(h_{11/2})^2$ pairs (H pairs) are used as the building blocks. The effective Hamiltonian consists of the single-particle energies and the P+QQ interaction, whose strengths are linearly changed as the number of valence neutrons.

Concerning the high-spin states, the backbending was experimentally observed at spin 10 for ^{134,136}Ce and at spin 12 for ^{132}Ce. Our calculation reproduced quite well the energy levels for the yrast bands, except for the level spacing between the 10_1^+ and 12_1^+ states of ^{134}Ce. Experimentally, the rapid drop of $B(E2)$ values occurred at the point of backbending for ^{134}Ce and ^{136}Ce, and the theoretical results exhibited the decrease of $B(E2)$ values between the 10_1^+ and 8_1^+ states. However, in ^{132}Ce backbending occurred at spin 12 while the $B(E2)$ value dropped at spin 10. We infer that the collective rotation delays the appearance of backbending. We also calculated g factors, and an excellent agreement with experimental values at spin 10 for ^{136,134}Ce was obtained. Experimental confirmation of our theoretical result is desirable for ^{132}Ce.

With respect to the low-lying states, good agreements between theoretical spectra and experimental data were achieved. Especially our results well described the staggering seen in 2_2^+, 3_1^+, 4_2^+ and 5_1^+ states in the quasi-γ band, which characterizes the γ-instability in low-lying states. The theoretical results of intraband and interband transition rates also agreed well with the experimental data. However the theoretical predictions did not succeed in reproducing the absolute $B(E2)$ values for the low-lying states. In the conventional collective models, it is quite difficult to produce the $B(E2; 4_1^+ \rightarrow 2_1^+)$ value which is smaller than the $B(E2; 2_1^+ \rightarrow 0_1^+)$ value, and there is a possibility that experimental absolute $E2$ transition strengths for all Ce isotopes are erroneous. More detailed measurements are expected to bring this controversy to an end.

The features of both low-lying and high-spin states were well interpreted in terms of the expectation values of the number of D and H pairs. The S and D collective pairs play essential roles in describing the low-lying states, while the effect of the alignment of two $0h_{11/2}$ neutrons becomes apparent above 10^+ states. We conclude that the truncation scheme extended to the SD+H subspace by including the intruder configurations provides an effective and minimal shell model space just enough to describe the yrast band, the γ-band and the backbending.

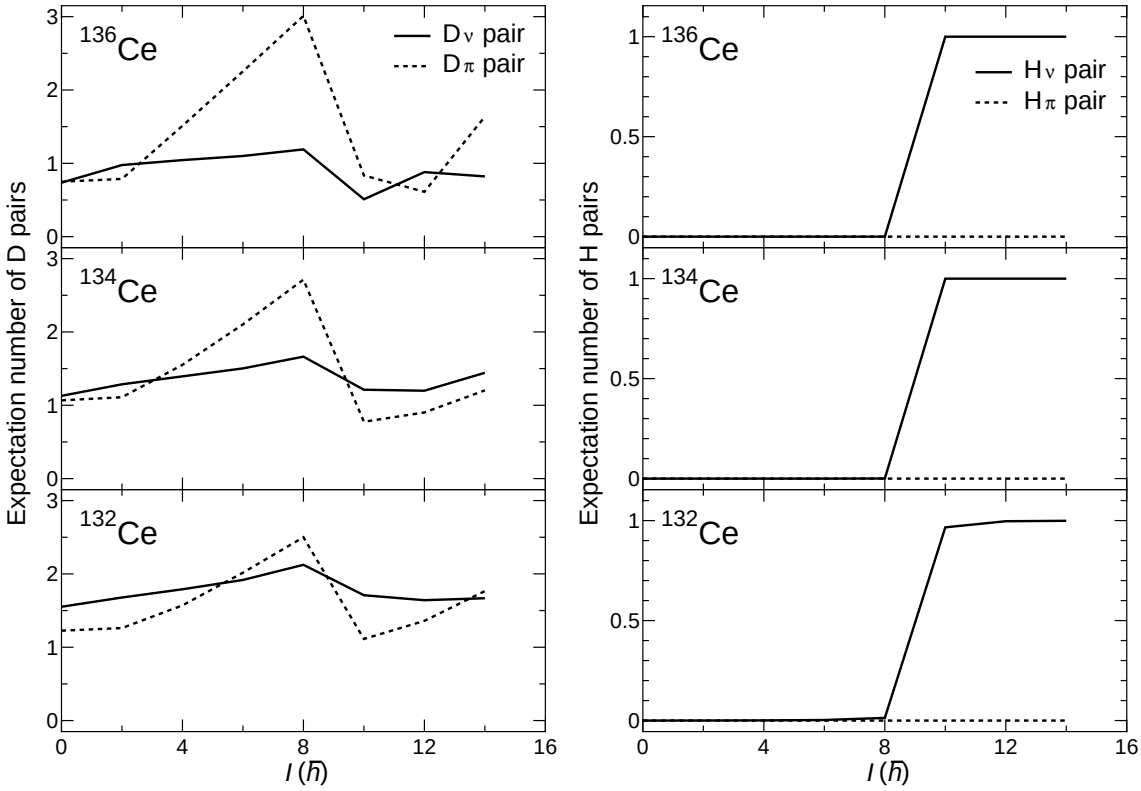

FIG. 7: The expectation numbers of D_τ pairs (left panel) and H_τ pairs (right panel) calculated in the PTSM for the yrast bands of ^{132,134,136}Ce. The solid line is for neutrons, and the dashed line for protons.

Acknowledgments

We would like to thank Professors K. Tanabe, N. Yoshida and A. Gelberg for their valuable discussions. One of the authors (K.H.) would like to thank JSPS Research Fellowships for Young Scientists.

[1] D. Husar, S. J. Mills, H. Gräf, U. Neumann, D. Pelte and G. Seiler-Clark Nucl. Phys. **A292**, 267 (1977).
[2] M. B. Goldberg, C. Broude, E. Dafni, A. Gelberg, J. Gerber, G. J. Kumbartzki, Y. Niv, K. -H. Speidel, and A. Zemel, Phys. Lett. **97B**, 351 (1980).
[3] H. Kusakari, K. Kitao, K. Sato, M. Sugawara, and H. Katsuragawa, Nucl. Phys. **A401**, 445 (1983).
[4] M. Muller-Veggian, H. Beuscher, D. R. Haenni, R. M. Lieder, and A. Neskakis, Nucl. Phys. **A417**, 189 (1984).
[5] A. Dewald, S. Harissopulos, G. Bohm, A. Gelberg, K. P. Schmittgen, R. Wirowski, K. O. Zell, and P. von Brentano, Phys. Rev. C **37**, 289 (1988).
[6] E. S. Paul, D. B. Fossan, Y. Liang, R. Ma, and N. Xu, Phys. Rev. C **40**, 1255 (1989).
[7] E. S. Paul, D. B. Fossan, Y. Liang, R. Ma, N. Xu, R. Wadsworth, I. Jenkins, and P. J. Nolan, Phys. Rev. C **41**, 1576 (1990).
[8] S. Juutinen, S. Tormanen, P. Ahonen, M. Carpenter, C. Fahlander, J. Gascon, R. Julin, A. Lampinen, T. Lonnroth, J. Nyberg, A. Pakkanen, M. Piiparinen, K. Schiffer, P. Simecek, G. Sletten, and A. Virtanen, Phys. Rev. C **52**, 2946 (1995).
[9] F. Iachello and A. Arima, *The Interacting Boson Model* (Cambridge University, Cambridge, 1987).
[10] S. G. Rohozinski, J. Dobaczewski, B. N. Pomorska, K. Pomorski, and J. Srebrny, Nucl. Phys. **A292**, 66 (1977).
[11] A. Gade, I. Wiedenhover, T. Diefenbach, A. Gelberg, M. Luig, H. Meise, N. Pietralla, M. Wilhelm, T. Otsuka, and P. von Brentano, Nucl. Phys. **A643**, 225 (1998).
[12] G. Puddu, O. Scholten, and T. Otsuka, Nucl. Phys. **A348**, 109 (1980).
[13] R. F. Casten and P. von Brentano, Phys. Lett. **152B**, 22 (1985).
[14] R. F. Casten, P. von Brentano, K. Heyde, P. Van Isacker and J. Jolie, Nucl. Phys. **A439**, 289 (1985).
[15] A. Sevrin, K. Heyde, and J. Jolie, Phys. Rev. C **36**, 2631 (1987).
[16] P. von Brentano, A. Gelberg, S. Harissopulos, and R. F. Casten, Phys. Rev. C **38**, 2386 (1988).
[17] X. W. Pan, T. Otsuka, J. Q. Chen, and A. Arima, Phys. Lett. B **287**, 1 (1992).
[18] T. Otsuka, Nucl. Phys. **A557**, 531c (1993).

[19] T. Mizusaki and T. Otsuka, Prog. Theor. Phys. Suppl. **125**, 97 (1996).

[20] O. Vogel, P. Van Isacker, A. Gelberg, P. von Brentano, A. Dewald, Phys. Rev. C **53**, 1660 (1996).

[21] N. V. Zamfir, W.-T. Chou, and R. F. Casten, Phys. Rev. C **57**, 427 (1998).

[22] C. L. Wu, D. H. Feng, X. G. Chen, J. Q. Chen, and M. W. Guidry, Phys. Lett. **168B**, 313 (1986).

[23] C. L. Wu, D. H. Feng, X. G. Chen, J. Q. Chen, and M. W. Guidry, Phys. Rev. C **36**, 1157 (1987).

[24] X. W. Pan, J. L. Ping, D. H. Feng, J. Q. Chen, C. L. Wu, and M. W. Guidry, Phys. Rev. C **53**, 715 (1996).

[25] N. Yoshinaga, Nucl. Phys. **A503**, 65 (1989).

[26] N. Yoshinaga and D. M. Brink, Nucl. Phys. **A515**, 1 (1990).

[27] N. Yoshinaga, Nucl. Phys. **A570**, 421 (1994).

[28] N. Yoshinaga, T. Mizusaki, A. Arima, and Y. D. Devi, Prog. Theor. Phys. Suppl. **125**, 65 (1996).

[29] N. Yoshinaga, Y. D. Devi, and A. Arima, Phys. Rev. C **62**, 024309 (2000).

[30] N. Yoshinaga and K. Higashiyama, Phys. Rev. C **69**, 054309 (2004).

[31] J. Q. Chen, Nucl. Phys. A626, 686 (1997).

[32] Y. A. Luo and J. Q. Chen, Phys. Rev. C **58**, 589 (1998).

[33] Y. M. Zhao, S. Yamaji, N. Yoshinaga, and A. Arima, Phys. Rev. C **62**, 014315 (2000).

[34] Y. A. Luo, J. Q. Chen, and J. P. Draayer, Nucl. Phys. **A669**, 101 (2000).

[35] K. Tanabe and K. Sugawara-Tanabe, Phys. Lett. **135B**, 353 (1984).

[36] K. Tanabe and K. Sugawara-Tanabe, Phys. Lett. B **259**, 12 (1991).

[37] K. Enami, K. Tanabe, and N. Yoshinaga, Phys. Rev. C **59**, 135 (1999).

[38] K. Enami, K. Tanabe, and N. Yoshinaga, Phys. Rev. C **61**, 027301 (2000).

[39] K. Higashiyama, N. Yoshinaga, and K. Tanabe, Phys. Rev. C **65**, 054317 (2002).

[40] K. Enami, K. Higashiyama, K. Tanabe, and N. Yoshinaga, Phys. Rev. C **66**, 047301 (2002).

[41] A. Gelberg and A. Zemel, Phys. Rev. C **22**, 937 (1980).

[42] N. Yoshida, A. Arima, and T. Otsuka, Phys. Lett. **114B**, 86 (1982).

[43] H. Kusakari and M. Sugawara, Z. Phys. **A317**, 287 (1984).

[44] A. Gelberg, N. Yoshida, T. Otsuka, A. Arima, A. Gade, A. Dewald, and P. von Brentano, in *Quasiparticle and Phonon Excitations in Nuclei (Soloviev 99)* edited by N. Dang and A. Arima (World Scientific, Singapore, 1999), p.100.

[45] K. Higashiyama, N. Yoshinaga, and K. Tanabe, Phys. Rev. C **67**, 044305 (2003).

[46] N. Yoshinaga and K. Higashiyama, in *Symmetries in Science XII* edited by B. J. Gruber (Kluwer Academic Publishers, 2004), p.589.

[47] S. Lakshmi, H. C. Jain, P. K. Joshi, Amita, P. Agarwal, A. K. Jain, and S. S. Malik, Phys. Rev. C **66**, 041303 (2002).

[48] S. Lakshmi, H. C. Jain, P. K. Joshi, A. K. Jain, and S. S. Malik, Phys. Rev. C **69**, 014319 (2004).

[49] A. J. Kirwan, G. C. Ball, P. J. Bishop, M. J. Godfrey, P. J. Nolan, D. J. Thornley, D. J. G. Love, and A. H. Nelson, Phys. Rev. Lett. **58**, 467 (1987).

[50] J. N. Wilson, G. C. Ball, M. Cromaz, T. E. Drake, S. Flibotte, A. Galindo-Uribarri, J. de Graff, G. Hackman, S. M. Mullins, J. M. Nieminen, V. P. Janzen, D. C. Radford, J. C. Waddington, and D. Ward, Phys. Rev. C **55**, 519 (1997).

[51] B. Fogelberg and J. Blomqvist, Nucl. Phys. **A429**, 205 (1984).

[52] M. Sanchez-Vega, B. Fogelberg, H. Mach, R. B. E. Taylor, A. Lindroth, J.Blomqvist, A. Covello, and A. Gargano, Phys. Rev. C **60**, 024303 (1999).

[53] W. J. Baldridge, Phys. Rev. C **18**, 530 (1978).

[54] L. S. Kisslinger and R. A. Sorensen, Rev. Mod. Phys. **35**, 853 (1963).

[55] A. Bohr and B. Mottelson, *Nuclear Structure* (Benjamin, New York, 1975) Vol.1.

[56] B. H. Ketelle, A. R. Brosi, and J. R. Van Hise, Phys. Rev. C **4**, 1431 (1971).

[57] A. Gade, I. Wiedenhover, M. Luig, A. Gelberg, H. Meise, N. Pietralla, V. Werner, and P. von Brentano, Nucl. Phys. **A673**, 45 (2000).

[58] E. S. Paul, A. J. Boston, D. T. Joss, P. J. Nolan, J. A. Sampson, A. T. Semple, F. Farget, A. Gizon, D. Santos, B. M. Nyako, N. J. O'Brien, C. M. Parry, and R. Wadsworth, Nucl. Phys. **A619**, 177 (1997).

[59] M. O. Kortelahti, B. D. Kern, R. A. Braga, R. W. Fink, I. C. Girit, and R. L. Mlekodaj, Phys. Rev. C **42**, 1267 (1990).

[60] D. Husar, S. J. Mills, H. Graf, U. Neumann, D. Pelte and G. Seiler-Clark, Nucl. Phys. **A292**, 267 (1977).

[61] W. Dehnhardt, S. J. Mills, M. Muller-Veggian, U. Neumann, D. Pelte, G. Poggi, B. Povh, and P. Taras, Nucl. Phys. **A225**, 1 (1974).

[62] S. Raman, C. W. Nestor, Jr., and P. Tikkanen, At. Data Nucl. Data Tables **78**, 1 (2001).

[63] H. J. Barth, G. Netz, K. Nishiyama, and D. Riegel, Phys. Rev. Lett. **45**, 1015 (1980).